ELECTRICAL BREAKDOWN CHARACTERISTICS OF SODIUM CHLORIDE - WATER MIXTURES

J. Bernardes and M. F. Rose
Naval Surface Weapons Center
Dahlgren, Virginia

Summary

The electrical breakdown characteristics of Na Cl-water mixtures are investigated over the concentration range from pure distilled water to a saturated salt solution at 20°C. The electrode material used is stainless steel and is arranged in a point-plane geometry. The electrode spacing is varied from 1-3 mm giving "average" electric fields as high as 5 MV/m. The voltage and current through the water are recorded as functions of time and used to calculate the conductivity of the mixtures as the breakdown progresses. The time delay between voltage application and catastrophic breakdown is measured as a function of the applied electric field and (electrode polarity). These data are analyzed in terms of possible breakdown mechanisms.

Introduction

The electromagnetics of water and water mixtures is of general interest for a wide range of technical applications in pulse power. Pure distilled, water is widely used for energy storage, pulse forming and electric field grading. The subject of breakdown in these "pure" solutions has been the subject of intense study since breakdown defines the limits of applicability, an if allowed to occur, can cause catastrophic damage.[1]

There is a second reason for studying breakdown in liquids. High voltage discharges, intentionally generated, form the basis of a number of industrial processes such as metal forming, solid breakup, switching, and geological prospecting.[2] Any solution in use very quickly becomes contaminated, with properties which vary depending upon the level of contamination. There is an extensive body of literature dealing with the electrical properties of pure-distilled water[3] and for the range of solutions normally used in industrial processes.[2] There is however very little data covering the conductivities associated with sea water.

Because of our interest in the electromagnetic of the ocean as it pertains to sonar, geophysical exploration, etc, we have conducted measurements of the breakdown properties of salt water solutions varying from zero percent salt to a saturated solution at room temperature.

Experimental

The pulse generator used in these experiments is shown in figure 1. It consists of a high voltage power supply which charges a capacitor bank through solenoid activated switches.

The capacitor bank consists of 4-35 μF capacitors (Sprague PQ 2535) arranged in a series/parallel matrix as shown. In the event of system failure, a 25 kΩ resistor, controlled from a console by means of the solenoid switch S_2, is inserted in the line, discharging the capacitor bank. To apply voltage to the test cell, switch S_3 is closed. Both current-time and voltage-time profiles are recorded on a single dual beam Tektronix 7844 oscilloscope using a rogowski coil and Tektronix high voltage probe respectively.
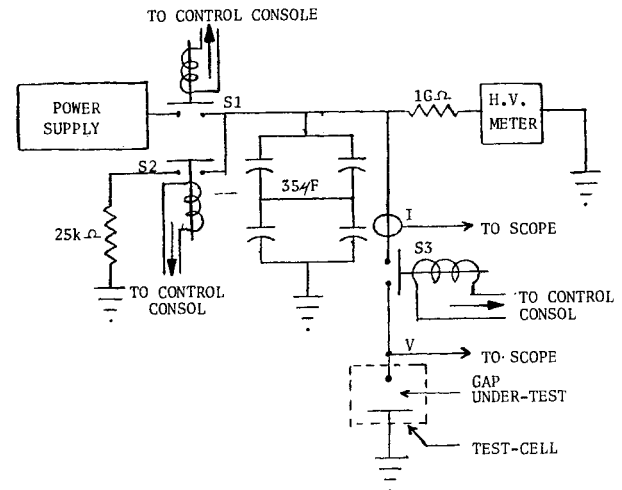

Figure 1. Schematic Diagram of Experimental Setup

In experiments of this type, it is necessary to keep the stray capacitance and inductance as low as possible. Wherever possible, a parallel plate geometry was used. The longest segment was 25 cm long and 12 cm wide. This segment connected the output gap (S_3 to the test cell. The output switch S_3, consists of a plate which is allowed to close over a 6.3 cm gap in the high voltage side of the transmission line. The gap is actuated by a solenoid device which brings the "striker" plate plane-parallel to the gap in the transmission line

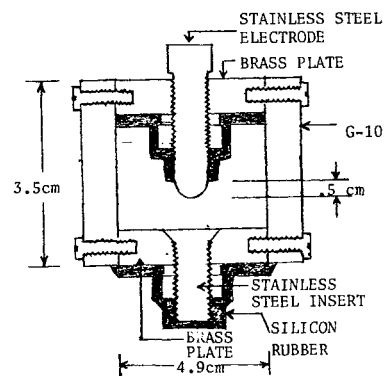The test cell assembly is shown in Figure 2.

Figure 2. Test Cell for Water Breakdown

Basically, the cell consists of a point-hemisphere-plane electrode geometry. The pointed electrode is made from stainless steel and is threaded to allow easy adjustment of the electrode spacing. The electrode is held in place by a brass plate and secured by stainless steel nut and washers. Similarly, the "plane" electrode is made from brass with a stainless insert. This was necessary because of erosion and the highly corrosive nature of the solutions used. When the system discharges, high dynamic stresses occur which

Report Documentation Page

1. REPORT DATE	2. REPORT TYPE	3. DATES COVERED
JUN 1983	**N/A**	**-**

4. TITLE AND SUBTITLE	5a. CONTRACT NUMBER
Electrical Breakdown Characteristics Of Sodium Chloride - Water Mixtures	5b. GRANT NUMBER
	5c. PROGRAM ELEMENT NUMBER

6. AUTHOR(S)	5d. PROJECT NUMBER
	5e. TASK NUMBER
	5f. WORK UNIT NUMBER

7. PERFORMING ORGANIZATION NAME(S) AND ADDRESS(ES)	8. PERFORMING ORGANIZATION REPORT NUMBER
Naval Surface Weapons Center Dahlgren, Virginia 22448	

9. SPONSORING/MONITORING AGENCY NAME(S) AND ADDRESS(ES)	10. SPONSOR/MONITOR'S ACRONYM(S)
	11. SPONSOR/MONITOR'S REPORT NUMBER(S)

12. DISTRIBUTION/AVAILABILITY STATEMENT
Approved for public release, distribution unlimited

13. SUPPLEMENTARY NOTES
See also ADM002371. 2013 IEEE Pulsed Power Conference, Digest of Technical Papers 1976-2013, and Abstracts of the 2013 IEEE International Conference on Plasma Science. Held in San Francisco, CA on 16-21 June 2013. U.S. Government or Federal Purpose Rights License.

14. ABSTRACT

15. SUBJECT TERMS

16. SECURITY CLASSIFICATION OF:			17. LIMITATION OF ABSTRACT	18. NUMBER OF PAGES	19a. NAME OF RESPONSIBLE PERSON
a. REPORT **unclassified**	b. ABSTRACT **unclassified**	c. THIS PAGE **unclassified**	**SAR**	**4**	

necessitate a design which will withstand repeated stressing. The brackets holding the test cell together were made from 1.8 cm G-10 and have successfully sustained many shots. In order to minimize conduction currents prior to breakdown, all exposed metallic surfaces except the point/plane area were coated with a silicon rubber compound.

The physical arrangement for the whole experimental assembly is shown in figure 3.The whole experiment as configured is approximately 13 in. x 21 in. x 14 in. and weighs about 50 pounds.
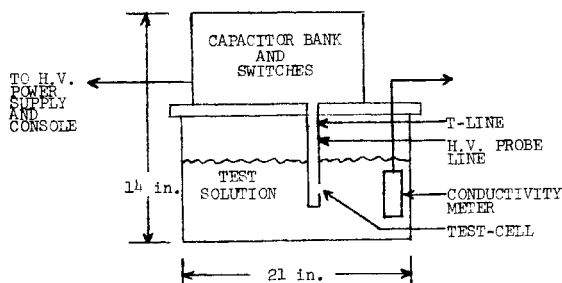

Figure 3. Experimental Assembly

In order to characterize the solution under test, a conductivity cell was designed to provide a ready and easy measurement of the electrical conductivity prior to experimentation. This cell is shown in figure 4. It consists of two cylindrical electrodes (r_1, r_2) of length L with nylon spacers and holes to allow the solution under test to penetrate the interelectrode space.
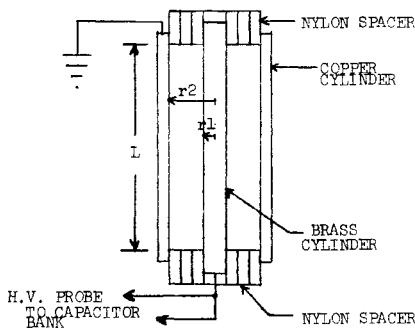

Figure 4. Conductivity Test Cell

In practice, a 1 kV pulse is applied to the submerged conductivity cell and the voltage decay as a function of time monitored. From this record, the RC decay is measured and R_c, the electrical resistance of the cell, calculated. The electrical conductivity (σ) is then:

$$\sigma = \ln \frac{r_2}{r_1} \Big/ 2\pi R_c L$$

Prior to an experimental run, temperature is monitored and all surfaces cleaned and coated.

Results and Discussion

There is a considerable amount of literature suggesting that the breakdown mechanism in liquid insulators is electronic in nature.[4] However, the level of understanding for strong and weak electrolytes is much less advanced due to the large number of ions which are capable of modifying the process. Various mechanisms have been proposed[2] based upon thermal, hydrodynamic, and ionization processes. None of these

are completely satisfactory and a detailed explanation must probably take into account all the above mechanisms.

The common features of all the existing experiments points to three distinct stages in the breakdown process. Stage I consists of the time from initial application of voltage until catastrophic breakdown begins to occur. Stage II, which is short lived and usually external circuit dominated, is that time when catastrophic failure occurs accompanied by a rapid decrease in the gap impedance. Stage III is the steady low impedance characterized by a fully developed arc and lasts as long as there is driving energy.

Figure 5 shows a typical trace from our experimental setup. The bottom trace shows I(t) and the top V(t) measured across the test cell. The current is roughly 3.7 kA/div and the voltage is 2 kV/div. The horizontal time scale is 5 μs/div.
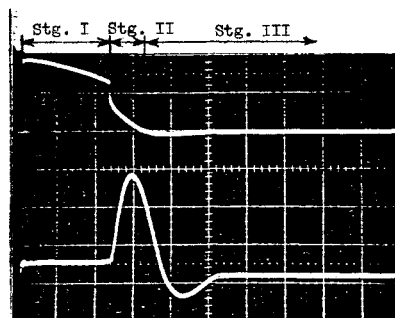

Figure 5. V(t) and I(t) for Test Cell.
t = 5μ s/div, V(t) = 2 kV/div, I = 3.7 kA/div, Cell Gap 3.0 mm, Resistivity = 15 Λ-cm

Table 1 summarizes the data taken for stage I.

TABLE I.
SUMMARY OF STAGE I

Sol. Resist. Ω-cm	Pt-Plane Gap mm	Init. Gap Resist Ω	Breakdown Field Mv/M	Maximum Applied Field Mv/M	Delay sec	Energy Dissipated Joules
10^5 Ω-cm	1.14	2800	2.7	4	$(1.6 \pm .48) \times 10^{-2}$	93
1.3×10^3	1.14	68.6	1.4	3.8	$(1.4 \pm .5) \times 10^{-4}$	32
	3.0	85.7	.86	1.4	$(3.6 \pm .3) \times 10^{-4}$	90
213	1.14	9.7	1.4	3.5	$(2 \pm .97) \times 10^{-5}$	41
	3.0	12.6	1.3	1.3	$(17 \pm 4) \times 10^{-6}$	215
15	1.14	.86	1 58	2.6	$(4 \pm .7) \times 10^{-6}$	46
	3.0	1.23	1.0	1.0	$(20 \pm 3.7) \times 10^{-6}$	235

The two parameters most of interest during this phase of the breakdown process are the delay time from the application of voltage to the beginning of impedance collapse (second stage) and the energy dissipated in the cell during this time. The voltage to which the capacitor bank is charged was held to 5 kV for all cases. However, at high conductivity, some of the energy stored in the bank was dissipated as the voltage increased on the test cell. The result is that for a given gap spacing, the maximum applied field is not constant. This is especially true for the solution whose resistivity is 15 Λ-cm. For the stated applied

field, the delay from voltage application to voltage collapse ranges from $(1.6 \pm .48) \times 10^{-2}$ sec for 10^5 Ω- cm distilled water to $(4 \pm .7) \times 10^{-6}$ sec for water/salt mixture of resistivity 15 Ω- cm. These numbers are quoted for the 1.4 cm gap. As the gap spacing is increased to 3.0 mm, a similar set of delay characteristics are observed.

For the external circuit parameters used, the spark discharge in the cell did not proceed along the minimum path length for 1.3×10^3 and 213 Ω- cm solutions. This was evident from direct observation of the event as well as the residual damage on the stainless steel insert in the anode.

A preliminary model to explain stage I behavior must incorporate pulse heating of the water/salt solution to high temperature. When bubbles form, breakdown begins to occur in much the same way as is observed in systems composed only of gasses. If this is true, the energy dissipated in the stage I should increase with gap spacing and with decreasing resistivity. These two trends are clearly evident from our experiment. It is useful to estimate the amount of energy necessary to evaporate a cylinder of water roughly equal in diameter to observed channels in water. For our minimum gap case, this estimate ranges from 30-100 joules, in good agreement with our experimental data. As the gap length increases, the discharge channel can "tree" and any calculation of this type becomes meaningless even for estimation purposes. Clearly, as the resistivity decreases, the ion currents increase and losses due to heating are greater. Increasing the gap spacing by roughly a factor 2.5 resulted in energy deposition in the cell increasing by factors of 3.5. In these expts. (for the 1.14 mm gap) the over voltage ranged from a factor of 2.71 to 1.65 while the energy dissipated in stage I increased only from 32 j to 46 j, only a 44% increase. By contrast for the larger gap, overvoltages from 1.63 to 1.0 produced losses from 90 joules to 235, an increase of a factor of 2.6.

In any application demanding efficient matching of energy to the load, Stage I must be minimized. Obviously, short gaps is one solution. A second would be to minimize the electrode surface exposed to solution in order to reduce prebreakdown conduction currents.

Stage II in the breakdown process is characterized by a sudden drop in the gap resistance as an arc is formed, figure 5, 6. The following more gradual voltage drop is roughly 5 μ s in time and is probably external circuit dominated. During this time, there is a rapid growth of current in the gap which will oscillate for a half or a full cycle, depending on arc length. This stage is associated with a fast dump of energy into the water which generates a strong shock wave.

The half cycle current oscillation (figure 6) is associated with a critical or overdamped response of the external circuitry and is evident only on the experiments which employed larger gap lengths with their resultant large arc length. For the shorter gap spacing, the current is observed to oscillate for one full cycle in an obvious underdamped condition. For all experiments conducted, the nature of the oscillatory behavior was independent of the solution resistivity but varied with the gap spacing. This implies that the final impedance reached in the collapse process is independent of the initial conductivity and governed solely by arc length as is the case for an arc in a gasseous discharge.

We modeled the experimental circuit as a series RLC arrangement and calculated the value of resistance necessary to produce critical damping. This value was found to be 120mΩ.. Further we analyzed several traces such as those shown in the figures above. For all cases, both visual observation and examination of the electrode damage shows the underdamped case to occur when the cell breaks down at the minimum gap spacing. Analyzing figures such as those above, give a value for the arc impedance of 20 mΩ/mm of arc length.
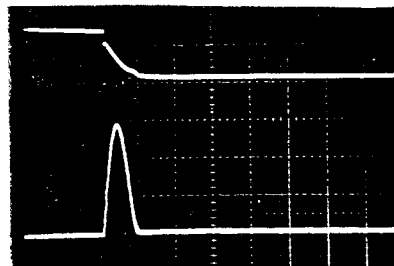

Figure 6. V(t) and I(t) for Test Cell showing Overdamped Response
t = 10 μs/div, V(t) = 2 kV/div, I(t) = 1.85 kA/div
Cell Gap = 3 mm, Resistivity = 213 Ω-cm

For the 1.3 kΩ-cm and the 213 Ω-cm solutions, both overdamped and underdamped responses were observed. In addition, for these cases, the spark initiation was observed to occur randomly over the cathode surface which, for a given minimum spacing, could result in arcs 3-5 times the minimum spacing. As a result, the amount of energy absorbed during stage II is erratic and is determined by the degree of damping and the spatial location of the arc.

Table 2 shows the average energy absorbed in the solutions as functions of gap spacing and circuit behavior.

Table 2.
ENERGY DEPOSITION DURING STAGE II

Resistivity Ω - cm	Electrode Spacing mm	Energy Deposition Joules	Circuit Behavior
1300	2.3	67	Mostly
	3.0	70	Overdamped
213	2.3	20	Mostly Underdamped
	3.0	45	Mostly Overdamped
15	2.3	22	Underdamped
	3.0	16	Underdamped

The maximum power input to the water occurs roughly 2 μs into the collapse of impedance. These values are typically—megawatts, and depend upon the water conductivity, gap spacing, how much energy was lost in stage I and the initial charge level for the capacitor bank.

Stage III is the steady state collapsed impedance of the cell which of course is maintained as long as there is driving energy to sustain that state. An average of our measurements indicates that the cell impedance in all cases collapses to a value, typical of breakdown in gasses and is on the order of 20 mΩ/mm. When the driving source is depleted, the cell impedance recovers in times on the order of .1 second.

A consistent model for our observations is shown in figure 7.
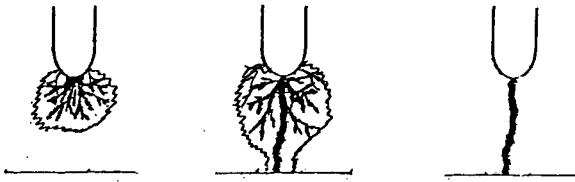
Stage I   Stage II   Stage III

Figure 7.   Stages in the Breakdown Process

In stage I, resistive heating of a fairly large
volume of the solution occurs. Since the field is not
uniform, selective heating at the anode/cathode in a
number of places may occur. In that localized region, a
gas bubble is formed which expands and greatly enhances
the breakdown process. In stage II, that gas/plasma
channel bridges the gap and results in impedance
collapse with the final stage (stage III) being typical
of the collapse in a gasseous media. As discussed in
the text, the exact details of each stage are influenced
by such parameters as solution conductivity, pulse rise
time, gap spacing, total energy in the pulses, etc.

References

(1)   P. S. Sincerny, "Electrical Properties of Water for
Repetitively Pulsed Burst Conditions," Proc 3 IEEE
International Pulsed Power Conference, June 1981,
Albuquerque, New Mexico.

(2)   High-Voltage Electrical Discharge in Pulse Power
Systems [Vysokovol'tnyy elektricheskiy razryad v
silovykh impul'snykh sistemakh] by G. A. Gulyy and P. P.
Malyushevskiy. Edited by G. A. ulyy, Kiev, "Naukova
Dumka", 1977.

(3)   Proc. 4th IEEE Pulsed Power Conferences, Session
XVII, "Water Dielectrics," Albuquerque, New Mexico, June
1983.

(4)   A. A. Vorobev et. al, "High Voltage Pulse Breakdown
and the Conductivity of Aqueous Electrolytes,"
Elektronnya Obrabotka Materialov, No. , 51-56, May-June,
1969.